Energy Conversion and Management 323 (2025) 119203

Contents lists available at ScienceDirect

Energy Conversion and Management

journal homepage: www.elsevier.com/locate/enconman

Research paper

Model benchmarking for PEM Water Electrolyzer for energy management purposes

Ashkan Makhsoos [a,b,*], Mohsen Kandidayeni [a], Meziane Ait Ziane [c], Loïc Boulon [a], Bruno G. Pollet [a,b]

[a] Hydrogen Research Institute (HRI), Department of Electrical Engineering and Computer Science, Université du Québec à Trois-Rivières (UQTR), 3351 boulevard des Forges, Trois-Rivières, Québec, G9A 5H7, Canada

[b] GreenH2Lab, Hydrogen Research Institute (HRI), Department of Chemistry, Biochemistry and Physics, Université du Québec à Trois-Rivières (UQTR), 3351 boulevard des Forges, Trois-Rivières, Québec, G9A 5H7, Canada

[c] Group of Research in Electrical Engineering of Nancy (GREEN), Université de Lorraine, Nancy, 54000, France

ARTICLE INFO

Keywords:
PEMWE
Electrochemical models
Energy management
Overpotential
Hydrogen production
Model benchmarking

ABSTRACT

This research conducts a comprehensive evaluation of various Proton Exchange Membrane Water Electrolyzer (PEMWE) models through a test bench, optimizing parameters and comparing obtained models against real-world data. Key operational factors such as reversible potential, activation overpotential, ohmic overpotential, and concentration overpotential are examined through experimental data. This study addresses critical gaps in current PEMWE research by reviewing modelling approaches, introducing a novel classification of models, and proposing an integrated approach that combines experimental validation with comprehensive model analysis. A novel, systematic methodology for model and submodel selection is presented, enabling practitioners to identify models that balance computational efficiency and predictive accuracy tailored to specific energy management and power allocation needs. This approach bridges the gap between complex modelling and industrial applications, enhancing the practical implementation of PEMWE systems in sustainable hydrogen production. Enhances model reliability for operational and manufacturing differences, provides invaluable guidance for improving the design and operation of these systems, and promotes a more robust and efficient hydrogen energy infrastructure.

1. Introduction

As the world continues to seek out sustainable energy sources, hydrogen is increasingly being viewed as a potential pathway for the future [1]. Hydrogen is a clean-burning fuel that emits only water vapour when burned, making it an attractive option for reducing greenhouse gas emissions [2,3]. Moreover, it can also be considered zero-emissions when it is utilized in Fuel Cells (FC) [4,5]. In addition to its role as a fuel, it is crucial in other industrial processes, including refining [6], steel production, and ammonia synthesis [7], demonstrating its versatility and essential role in a variety of industrial processes [8]. However, the challenges of hydrogen production and storage remains a significant barrier to widespread adoption [9,10]. One promising technology in this regard is the Proton Exchange Membrane Water Electrolyzer (PEMWE), which utilizes renewable energy sources (RES) such as solar, wind, or hydro power to produce green hydrogen from water [11,12]. PEMWE is a popular choice for hydrogen production due to its high operational efficiency in low operating temperatures [13]. Furthermore, the scalability of PEMWE systems is a significant advantage, allowing for flexible adjustments in capacity to meet diverse application requirements [14,15].

PEMWE's installed capacity has grown significantly between 2019 and 2023, and this issue is depicted in Fig. 1. According to predictions, the pace of this growth will continue to accelerate in the coming years [16]. The growth of hydrogen production in megawatt (MW) and gigawatt (GW) scale has become increasingly important in recent years due to the need for sustainable energy patterns and the drive towards achieving zero-emission goals [17]. The use of modular structures and power allocation strategies has become essential for efficient green hydrogen production in large-scale applications. These modular structures allow for easy scalability of the system and enable the efficient allocation of power based on the fluctuating demand for hydrogen production. Effective energy management is also crucial for the efficient operation of large-scale hydrogen production systems. The optimization of parameters such as operating current density, temperature, water

* Corresponding author.
E-mail address: ashkan.makhsoos@uqtr.ca (A. Makhsoos).

https://doi.org/10.1016/j.enconman.2024.119203
Received 4 September 2024; Received in revised form 17 October 2024; Accepted 25 October 2024
Available online 11 November 2024

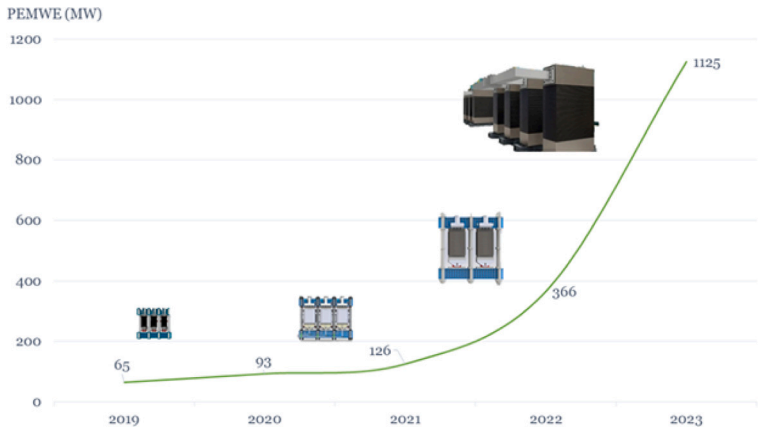

Fig. 1. The total installed capacity of PEMWE in the last four years [20].

and air flow rates, and material selection can significantly improve the energy efficiency of the system, reduce operating costs, and increase the overall sustainability of hydrogen production [18,19].

As the usage of large-scale PEMWEs increases, it becomes imperative to have accurate and practical models for them and algorithms for feeding electrolysers which can affect the behaviour of these systems across different scales [21]. The development of such models can facilitate a better understanding of PEMWE's behaviour and enable efficient design, operation, and control of these systems [22]. It is particularly relevant to increase PEMWE's scale using giant stacks or modular designs. Despite the challenges, modelling studies are crucial to developing efficient and effective electrolyzer systems for hydrogen production. Accurate models can provide insights into maximizing production, minimizing degradation, and increasing system lifespan [23]. Therefore, developing reliable and scalable models for PEMWE inputs (energy and water) is crucial to enable widespread adoption and unlock their potential as a critical technology for sustainable energy conversion and storage [24].

PEMWE modelling reviews are crucial for assessing current models, highlighting strengths, weaknesses, and research needs [25]. Lamy and Millet's analysis of energy efficiency in water electrolysis cells underscores the importance of these coefficients for evaluating performance and cost-effectiveness [26]. Olivier et al. offer an overview of low-temperature electrolysis, including PEM and alkaline, identifying key research areas and using a comparative approach [27]. Falcao and Pinto focus on PEM electrolyzer modelling, discussing prediction equations for cell voltage and performance expectations [28]. Hernandez-Gomez et al. explore the electrical aspects of PEMWEs, suggesting empirical models to enhance electrolyzer performance [29]. Majumdar et al. discuss dynamic models and control techniques for PEMWEs, stressing the significance of data-driven models and degradation-aware control algorithms [30].

Effective energy management within PEMWE systems is paramount, not only to optimize performance but also to ensure economic viability and environmental sustainability [31]. Integrating intelligent Energy Management Systems (EMS) that can dynamically adjust to varying renewable energy inputs and operational demands is crucial [32,33]. These systems help balance hydrogen production rates and energy consumption, optimizing overall efficiency and reducing costs. However, selecting the appropriate models for these EMSs can be challenging due to the many available models, each with its strengths and weaknesses [34]. Selection becomes even more complex when considering the variations and iterations within a single type of model. Various models can provide different insights and results, which can significantly affect the understanding of PEMWE system performance and consequently decision-making in EMS.

This diversity of models creates a special issue when determining which model is most appropriate for a certain application. The choice of model affects not only the accuracy of predictions and optimizations but also the practical feasibility of implementing solutions at scale. Given that every system has its character, operational condition, and performance metrics, it is not feasible to universally recommend a single model as the optimal choice across different systems. To address this challenge, introducing a systematic method for comparing and choosing a benchmark model tailored to each specific system could prove invaluable. Researchers seeking the most appropriate models for energy management and power allocation as well as industry professionals seeking robust, application-specific models would benefit from this approach.

Prior research has explored various PEMWE models, including complex multidimensional analyses [24], integration with RES [31–33], and control-oriented methods [30,34]. Other studies have examined temperature-dependent models to assess operating condition impacts [27,35,36] and employed simulations to investigate PEMWE behaviour under diverse scenarios [25,37–39]. While electrical domain models focus on efficiency and energy consumption [29,37,40], empirical studies gauge hydrogen production rates and system efficiencies [29,37,39,41,42], demonstrating the broad array of modelling techniques in use [28,43,44].

Despite these developments, there is a notable lack of comprehensive comparison or benchmarking among models tailored for PEMWE applications, a gap this study aims to fill. It benchmarks a wide array of electrochemical models, providing a structured framework to assess their complexity, performance, and applicability to energy management—critical for enhancing green hydrogen production at scale. This study addresses existing gaps in PEMWE research by conducting a comprehensive evaluation of modelling approaches geared towards power allocation and energy management. It introduces a novel classification of models and integrates rigorous experimental validation with in-depth analytical review, offering practitioners a method to select and validate models that balance computational efficiency with predictive accuracy, tailored to unique system requirements.

In summary, this paper provides essential comparisons and guidelines for model selection, substantially aiding the advancement of large-scale green hydrogen production through refined PEMWE modelling strategies.

This research aims to establish a practical method for selecting an appropriate model among the myriad available, tailored to the unique characteristics and operational conditions of each system. Section 2 provides a rapid analysis of model types and introduces the domains of PEMWE from an energy management perspective. Section 3, aligned with energy management principles, selected overpotentials are chosen, and a novel method for comparing and selecting the most appropriate models is introduced. Section 4 describes a test bench setup developed for validation and for comparing theoretical predictions with practical outcomes. Section 5 presents the test bench used for models

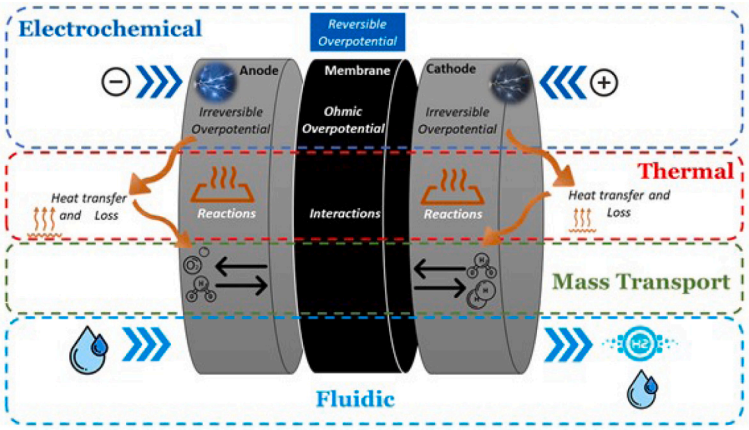

Fig. 2. Coupling of different domains for PEMWE modelling.

validation. Section 6 presents the results and discussions, providing a comprehensive evaluation of the proposed methodology.

2. PEMWE models for energy management

A PEMWE consists of interconnected domains: electrochemical, mass transport, fluid flow, and heat transfer, as shown in Fig. 2. Changes in one domain affect others, necessitating coupled sub models. In electrochemical reactions, the anode and cathode are involved, and catalysts play a role in these reactions. Overpotentials and voltage losses influence these reactions. Mass transport involves the diffusion and convection of reactants and products through the membrane and gas diffusion layers, requiring accurate modelling of species distribution and concentration profiles. Fluid flow involves water supply to the anode and gas generation, with models considering flow rates and pressure differentials [45]. Heat transfer involves thermal effects from electrochemical reactions, requiring models for heat generation and loss.

Understanding electrolyzer performance through polarization and voltage modelling is crucial for energy management. The cell voltage provides insights into hydrogen production efficiency. Variations in voltage can help identify different modes of operation, assess ageing, and determine degradation rates. It is first necessary to determine the cell voltage, considering voltage and overvoltage. Although this section primarily focuses on energy management, all domains indirectly impact overvoltage and are considered in experimental tests. The primary direction is electrochemical analysis.

PEMWE behaviour is complex, with changes in one domain impacting others. Coupled sub-models in physics-based models are essential. For example, electrochemical performance variations affect species concentration and transport, while fluid flow adjustments alter reactant and product concentrations. Thermal effects influence electrochemical kinetics and species transport properties. Accurate simulation requires integrated models to capture these interactions. As this complex phenomenon is approached from a variety of perspectives, it becomes important to adopt a modelling approach.

Models that link the practical operational system with various parameters and variables underpin PEMWE's EMSs. Several factors, such as hydrogen production rates and overall system efficiency, require the implementation of models that can accurately predict and manage these factors, such as voltage models. Various modelling approaches exist, each with distinct strengths and weaknesses, categorized based on the level of understanding of the system's physical or mathematical structure. Determining the superior model type — whether empirical, theoretical, or mathematical — hinges on the specific requirements and constraints of the PEMWE system.

As shown in Fig. 3, three primary modelling categories can be distinguished: white box, grey box, and black box. Empirical models, or black-box models, are constructed based on experimental data and observations. In general, they require fewer computational resources and are easier to develop but may not generalize beyond specific conditions. Theoretical mathematical models, or white-box models, are built on underlying physical and chemical principles and offer insights into the internal workings of the system. These models can be extrapolated to different operating conditions but are often complex and computationally demanding. Grey-box modelling, combining elements of both empirical and theoretical approaches, is particularly suitable for energy management in PEMWEs where both predictive accuracy and computational efficiency are critical. Thus, grey-box modelling is a preferable strategy for effective energy management in PEMWE systems, offering a pragmatic blend of detail and applicability.

For finding electrochemical voltage equation PMWE overall reaction, which is illustrated in (1), can be the first step. It shows how water is split into hydrogen and oxygen [43]

$$2H_2O \rightarrow O_2 + 2H_2 \tag{1}$$

This reaction occurs at the electrodes: the anode handles the OER given by (2) and the cathode handles the HER expressed by (3)

$$2H_2O \rightarrow O_2 + 4H^+ + 4e^- \tag{2}$$

$$4H^+ + 4e^- \rightarrow 2H_2 \tag{3}$$

In a PEMWE cell, water splits into hydrogen and oxygen (1), requiring electricity for electrolysis. The standard reversible cell voltage, $V_{(rev,s)}$ can be calculated by considering the maximum heat energy input of 48.6 kJ/mol, as outlined in (4) [46]

$$V_{rev,s} = \frac{\Delta G}{n_e F} = 1.23\,V \tag{4}$$

where the change in Gibbs free energy (ΔG) is 237.22 kJ/mol for the reaction, n_e the number of electrons transferred, typically 2 for water splitting and F is the Faraday constant, approximately 96485 C/mol, representing the charge of one mole of electrons.

The theoretical voltage V_{th} for water splitting in a PEMWE cell can be calculated using the enthalpy (ΔH) which is expressed by

$$\Delta H = \Delta G + T\Delta S \tag{5}$$

where T is the cell temperature in Kelvin and (ΔS) is the entropy change. Under standard conditions, the change in enthalpy (ΔH) is 285.84 kJ/mol. Using this information, the minimum voltage for water electrolysis, represented as V_{th} can be calculated as follows [41]

$$V_{th} = \frac{\Delta H}{n_e F} = 1.48\,V \tag{6}$$

The cell voltage V_{cell} is determined by taking into account various losses in a PEMWE system, additional considerations are required. These voltage losses should be added to reversible voltage V_{rev} to result

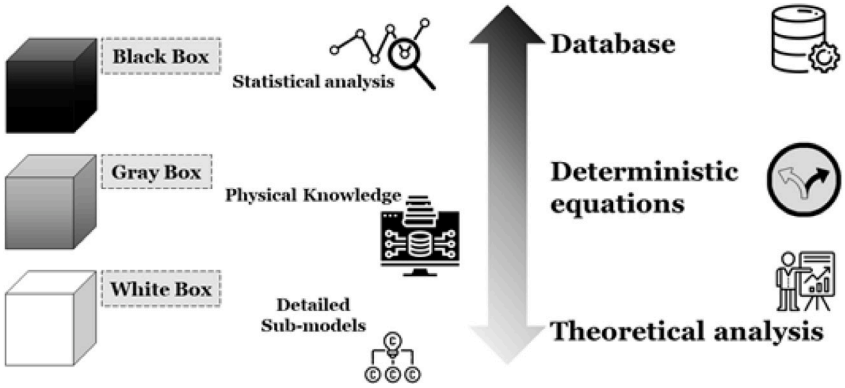

Fig. 3. Different types of models from the point of view of origin.

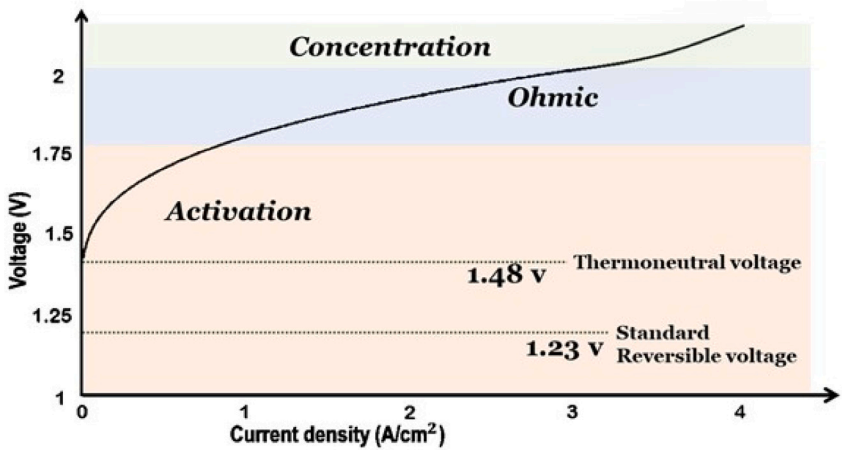

Fig. 4. PEMWE cell polarization curve [49].

in an approximation of cell voltage. By considering the four major voltage loses, the cell voltage V_{cell} is expressed by [47]

$$V_{cell} = V_{rev} + U_a + U_o + U_c + U_b \tag{7}$$

where U_a is concentration losses, U_o is ohmic losses, U_c is concentration losses and U_b is bubble overpotential.

Activation losses U_a arise from the high activation energy needed for electrochemical reactions at the electrodes, reducing efficiency. Ohmic losses U_o, due to the electrolyte's resistance and ion movement, are a primary source of irreversibility. Concentration losses U_c result from reactant and product concentration gradients, affecting mass transport within the cell. Bubble overpotential U_b models the irreversibility of bubble formation at the electrodes and membrane. While these losses increase overall voltage, researchers may focus on specific losses based on their model's complexity. Sometimes, only activation and ohmic losses are considered for simplicity [48].

A PEMWE cell polarization curve, shown in Fig. 4, illustrates the relationship between cell voltage and current density during water electrolysis. This curve is crucial for assessing the system's efficiency and performance, helping researchers identify voltage losses and determine optimal operating conditions.

The variable quantity of HyPro can be described using (8)

$$\text{HyPro} = \int_0^t f_{H_2} \mathrm{d}t = \frac{\int_0^t N.I.V.\eta_e.\mathrm{d}t}{HHV_{H_2}.\rho_{H_2}} \tag{8}$$

where N is the number of cells, and η_e is the PEMWE efficiency determined by (9), which is linked to the current [44,50].

The higher heating value of hydrogen HHV_{H_2} is a crucial thermodynamic property indicating the energy liberated when hydrogen is combusted, quantified here as approximately 39 400 J/g. The density of hydrogen, ρ_{H_2} under standard conditions is around 0.8988 g/L.

The energy efficiency coefficient of water electrolysis η_e can be calculated in function of current by [50]

$$\eta_e = -0.0786I^3 + 1.167I^2 - 7.365I + 84.44 \tag{9}$$

3. Overpotential model selection for a PEMWE

A balance is achieved between transparency and flexibility in this study of PEMWE by using grey box models. They provide a satisfying balance between the comprehensiveness of white box models and the simplicity of black box models by integrating theoretical principles with empirical data. A focus is placed in this section on the precision modelling of voltages applied to electrodes, a critical factor in considering energy management and power allocation in PEMWE systems. The voltage across a PEMWE cell, designated as V_{cell} in (7), is subject to various losses and irreversibility. These influences, along with diverse modelling strategies documented in the literature, are comprehensively examined. Moreover, the section emphasizes that models should be designed with a balance of simplicity and adaptability, ensuring they are both easy to integrate into the system and sufficiently accurate for the goal of efficient energy management. The focus is on achieving fast and straightforward operation while maintaining a high degree of precision in tracking and responding to real-time conditions. Such adaptability not only aligns with ongoing technological developments but also supports the integration of PEMWE systems into broader energy frameworks, thereby enhancing scalability and operational efficiency. This discussion sets the stage for subsequent sections, which will compare experimental outcomes with theoretical predictions, further

analysing and optimizing various identified models based on their operational parameters and utility.

3.1. Reversible potential

A PEMWE's reversible potential voltage is the minimum voltage required to initiate it from a thermodynamic standpoint. It is common for studies to take into consideration the constant reversible voltage, typically around 1.229 V at standard temperature and pressure as it is called standard reversible voltage $V_{rev,s}$ as shown in (4). Reversible standard voltage $V_{rev,s}$ is sometimes called reference voltage or standard voltage and is expressed in various forms E^0_{rev}, E_0 or V_0 and also is calculated through different simple and complicated formulas [37]. The standard reversible potential represents an ideal scenario under standard conditions.

In contrast, the reversible potential in PEMWE reflects actual operating conditions, incorporating variations such as temperature, pressure, and reactant concentration. Various equations in the literature estimate this potential, each varying in complexity and operational detail. The empirical linear model simplifies calculations by directly correlating voltage to deviations from the standard temperature of 298 K, making it practical and predictable for conditions close to the norm but less effective outside this range. Conversely, the thermodynamic integral-based approach caters to a more extensive temperature spectrum, though its reliance on comprehensive data adds complexity.

Other strategies include polynomial models which, by incorporating terms up to T^3, effectively manage higher-order temperature impacts but increase computational demands. Linear models provide ease and efficacy under near-standard conditions but falter when broader applicability is required. The logarithmic model offers a mid-ground by balancing simplicity with a detailed representation of non-linear temperature effects, although its accuracy may diminish at extreme values.

Enhanced adaptability to varied operational scenarios is achieved by adding additional models that consider temperature, pressure, enthalpy, and entropy, or that utilize reference pressures. Selecting the right model balances computational efficiency with the precision required for PEMWE systems, ensuring alignment with operational demands and energy management limitations. Among them (10) stands out for its effective balance between simplicity and complexity, making it particularly suitable for practical energy management applications. It efficiently integrates key parameters, enabling quick and accurate calculations of cell voltage under non-standard conditions. By using logarithmic terms to account for pressure and concentration effects, (10) offers a tailored approach to the dynamic environments of PEMWEs. Furthermore, the factors considered in this formula such as temperature and pressure are typically measured within an energy management system, aligning with practical application needs [51].

$$V_{rev} = V_{rev,s} + \frac{RT}{2F} \times \ln\left(\frac{P_{H_2} P^{0.5}_{O_2}}{\alpha_{H_2 0}}\right) \tag{10}$$

where water activity $\alpha_{H_2 0}$ assumed to be 1, R is universal gas constant, and P_{H_2} is partial pressure of hydrogen and P_{O_2} is partial pressure of oxygen; and also the standard potential $V_{rev,s}$, which is represented by (4) and can be calculated accordingly [52].

3.2. Activation overpotential

In PEMWE electrochemical modelling, activation overpotential is the extra voltage required to initiate an electrochemical reaction at the electrode–electrolyte interface. It drives a Faradaic current and decreases with rising operating temperature due to increased exchange current density, which enhances the reaction. This overpotential arises from kinetic barriers such as reactant adsorption/desorption, charge transfer, and reactant diffusion. Factors influencing it include temperature, pressure, catalyst activity, and reactant concentration. Understanding activation overpotential helps optimize PEMWE design and operation, improving performance and energy efficiency, crucial for energy conversion and storage applications.

Activation overpotential, U_a reflects the reaction rate and consists of anode $U_{a,a}$ and cathode $U_{a,c}$ components as shown in (11). Some studies consider the cathode side negligible [35]. Each of the anode and cathode can be placed in place of j and the formulas from (121) to (14) can be personalized for each. calculate these overpotentials, applicable to oxidation at the anode and reduction at the cathode. This concept links the electrical current through an electrode to the voltage difference between the electrode and electrolyte for a single-molecule redox reaction involving both anodic and cathodic reactions. Various U_a equation forms exist in the literature shown in Table 1 along with their estimated computational speed.

One of the widely used expressions for calculating activation overpotential U_a is (12), which has been employed by numerous authors in the development of electrolysers models [53]. The parameter α is the symmetry factor that accounts for the additional energy fractions involved in the reduction (anode) and oxidation (cathode) processes. i_j represents the current density at the jth electrode, which is a measure of the electric current per unit area of the electrode. $i_{0,j}$ refers to the exchange current density at the jth electrode, indicating the rate of the electrochemical reaction when there is no net current flow (i.e., when the electrochemical reaction is at equilibrium). In (13), z represents the stoichiometric coefficient of the number of electrons involved. The rugosity factor γ_j in (14) represents the effective surface area of the electrode in relation to its geometric area, accounting for the microstructural characteristics and porosity [54]. (15) uncovers the effects of double-layer capacitors with shunt capacitors $C_{dl,j}$. In this equation, the current density flowing through the PEMWE stack is represented by i. The parameters ρ_j and τ_j are determined based on empirical functions that correlate to temperature.

3.3. Ohmic overpotential

Overpotential in the PEMWE electrochemical model refers to the resistance to electric current flow. It is linked to the ionic conductivity of the electrolyte and resistance of cell components, including electrodes, current collectors, and membranes. An external voltage is applied to drive the electrochemical reaction, but a voltage drop, called ohmic overpotential U_o, occurs due to resistance, reducing the effective potential for reactions. Ohmic overpotential U_o can be mathematically described using Ohm's Law, where the voltage drops U_o is equal to the product of the current density i and the total equivalent resistance Ω_{eq} in the system as illustrated in (16). Two frequent equations in the literature are shown in Table 2.

The equivalent resistance Ω_{eq} includes contributions from the electrolyte's ionic conductivity, the membrane's thickness and conductivity, and the contact resistance at the interfaces between the electrodes and the current collectors. These factors collectively determine the Ohmic overpotential in the PEMWE system. A good approximation of this equivalent resistance is the resistances of membrane Ω_M and electrodes Ω_E which is given by

$$\Omega_{eq} = \Omega_M + \Omega_E \tag{18}$$

According to (18), Ω_E stands for electrical resistance in electrodes. Membrane resistance Ω_M is given by

$$\Omega_M = \frac{\theta}{\mathfrak{V}} \tag{19}$$

where θ is the thickness of the membrane and $\mathfrak{V}$ represents the conductivity of the membrane expressed as follows

$$\mathfrak{V} = (0.005139\lambda - 0.00326)\exp\left(1268 \times \left(\frac{1}{303} - \frac{1}{T}\right)\right) \tag{20}$$

where λ refers to membrane humidification [59].

Table 1
Different versions of the literature's activation overpotential equations.

Equations		Parameters involved	Computational speed
$U_a = U_{a,a} + U_{a,c}$	(11)	Anode and cathode potentials	Fast
$U_{a,j} = \frac{RT_j}{\alpha_j F} \sinh\left(\frac{i_j}{2i_{0,j}}\right)^{-1}$	(12)	Temperature, symmetry factor and current density	Moderate
$U_{a,j} = \frac{RT_j}{z\alpha_j F} \sinh\left(\frac{i_j}{2i_{0,j}}\right)^{-1}$	(13)	Includes valence	Moderate
$U_{a,j} = \frac{RT_j}{z\alpha_j F} \ln\left(\frac{i_j}{\gamma_j i_{0,j}}\right)^{-1}$	(14)	Rugosity factor	Moderate
$\frac{dU_{a,j}}{dt} = \frac{\rho_j}{C_{dl,j}}\left(1 - \exp\left(\frac{U_{a,j}}{N\tau_j}\right)\right) + \frac{i}{C_{dl,j}}$	(15)	Dynamic components including capacitance and resistance	Very slow

Table 2
Ohmic overpotential formulas in scholarly works.

Ohmic overpotential equations		References
$U_o = i \times \Omega_{eq}$	(16)	[41,52,55–57]
$U_o = i \times \Omega_M$	(17)	[35,37,38,58]

Table 3
Distinct concentration overpotential formulas in scholarly works.

Concentration overpotential equations		References
$U_{c,j} = \frac{RT}{Z_j F} \ln\left(\frac{con_j}{con_{j,0}}\right)$	(21)	[36,42,56,64–67]
$U_c = \frac{RT}{\beta ZF} \ln\left(1 + \frac{i}{i_l}\right)$	(22)	[55,58]
$U_c = i\left(\beta_1 \frac{i}{i_l}\right)^{\beta_2}$	(23)	[68]
$U_c = \frac{RT}{\beta ZF} \ln\left(\frac{\frac{i}{i_l}}{1-\frac{i}{i_l}}\right)$	(24)	[39,64]

Additionally, there are other approaches to calculation that include more details and can be chosen for various applications or research but are not necessary for energy management purposes. For instance, Correa et al. [60] note that membrane conductivity is influenced by its prior state, the activation energy for proton transport, and temperature [40]. Jing et al. [61] discuss the concept of equivalent resistance, which is calculated based on the area-specific resistance and the cell's surface area [62]. This resistance is impacted by various factors including temperature, with different components of the electrolysis cell showing varying degrees of temperature dependency [63].

3.4. Concentration overpotential

Concentration overpotential, labelled U_c, results from concentration gradients at electrodes during electrochemical processes like PEMWE water electrolysis. It increases due to mass transport issues, leading to higher energy use, lower efficiency, and more operating costs. This phenomenon also causes uneven current distribution and pH changes, which affect electrode life and stability. U_c sums up the individual overpotentials at the anode $U_{C,a}$ and cathode $U_{C,c}$.

The Nernst equation calculates concentration over potential as shown in (21) in Table 3. It uses con_j to denote the concentration of oxygen at the anode or hydrogen at the cathode, depending on whether $\varepsilon j\, \varepsilon$ equals $\varepsilon a\varepsilon$ or $\varepsilon c\varepsilon$ [37]. $con_{j,0}$ represents the reference concentrations of oxygen and hydrogen at the anode and cathode, respectively. Stoichiometric coefficients vary, with z_a being 4 at the anode and z_c being 2 at the cathode.

In literature, an alternative model for calculating the concentration overpotential is described by (22), which involves an empirically derived coefficient represented as β and the limiting current density i_l are determined by the diffusion capabilities. Based on the experimental data mentioned in [69], these specific values were obtained through curve fitting. The concentration overvoltage in PEMWEs can also be described by a model that incorporates the limiting current density i_l in (23). In this model, the coefficient β_1 is dependent on oxygen pressure and temperature, while β_2 remains constant. As noted in (24), bubble overpotential is sometimes included in concentration overvoltage studies. A limiting current density i_l causes bubbles to form, resulting in efficiency losses. At low current densities, concentration overpotential is often neglected due to the prominence of ohmic and activation overpotentials. However, its impact can vary significantly depending on the system's parameters and conditions [66]. To mitigate concentration overpotential and improve PEMWE performance, strategies focus on enhancing mass transport, optimizing flow fields, increasing electrode surface area, and selecting high-activity, stable catalysts to improve reaction kinetics and reduce overpotential.

Bubble overpotential U_b arises when gas bubbles, mainly hydrogen, accumulate on the electrode surface during electrolysis, impeding reactant transport and lowering electrochemical activity. This phenomenon is influenced by current density, electrolyte composition, and electrode design. High current densities or low reactant concentrations can worsen this effect, leading to increased polarization and reduced cell performance [70]. While some studies treat bubble overpotential as negligible, others acknowledge its role, particularly in non-uniform gas bubble distribution and the disruption of fluid flow patterns, which reduce mass transport and performance. In some models, bubble effects are considered by adjusting Butler–Volmer equations to incorporate nonlinearity; however, these considerations are not always considered in the context of broader system models. Ex-situ and system-wide models often overlook bubble overpotential despite its significance in some contexts [71].

4. Towards tailored overpotential model selections in PEMWE systems

The study utilized a systematic method to identify the most effective electrochemical model from eight variations (M_1 to M_8), each defined by different overpotential combinations. The identified eight models are expressed as follows

$$M_1 = V_{rev} + U_{a,1} + U_{o,1} + U_{c,1} \quad (25)$$

$$M_2 = V_{rev} + U_{a,1} + U_{o,1} + U_{c,2} \quad (26)$$

$$M_3 = V_{rev} + U_{a,1} + U_{o,2} + U_{c,1} \quad (27)$$

$$M_4 = V_{rev} + U_{a,1} + U_{o,2} + U_{c,2} \quad (28)$$

$$M_5 = V_{rev} + U_{a,2} + U_{o,2} + U_{c,1} \quad (29)$$

$$M_6 = V_{rev} + U_{a,2} + U_{o,2} + U_{c,2} \quad (30)$$

$$M_7 = V_{rev} + U_{a,2} + U_{o,1} + U_{c,1} \quad (31)$$

$$M_8 = V_{rev} + U_{a,2} + U_{o,1} + U_{c,2} \quad (32)$$

Table 4
Overpotential models selection for energy management in PEMWE systems.

Overpotentials	Abb	Eqs	Parameters: All/Known constant/Estimated/Measured	Rationale/Notes
Reversible	V_{rev}	(10)	7/5/1/1	Balances precision and responsiveness
Activation	$U_{a,1}$	(13)	7/3/2/2	Known temperature relationships
Activation	$U_{a,2}$	(14)	8/3/3/2	Current interplays
Ohmic	$U_{o,1}$	(16)	3/0/2/1	General applicability
Ohmic	$U_{o,2}$	(17)	4/0/2/2	Requiring comprehensive modelling
Concentration	$U_{c,1}$	(22)	7/3/2/2	Known limiting currents
Concentration	$U_{c,2}$	(23)	4/0/3/1	Non-linear response traits

Table 4 compares sub-models' side-by-side, highlighting their composition, parameters, and approach. This comparative analysis not only assessed each model's accuracy against experimental data but also their computational needs and practicality. Although this method provides a framework for selecting appropriate models for various electrolyzers, it should be noted that it proposes a hypothesis rather than conclusive results, serving as a preliminary guide in model selection across different scenarios.

Striking an optimal balance between computational efficiency and parameter detail is crucial in selecting sub-models for each component of these eight electrochemical models. Unlike other models, where two are chosen for comparison, the reversible overpotential V_{rev} specifically employs the logarithmic temperature–pressure dependency model. This model is well-documented in the literature and is an effective choice from an energy management perspective, particularly in controlled systems where pressure and temperature are routinely monitored.

The comparative analysis of (13) and (14) highlights their integration of critical parameters within electrochemical model benchmarking. (13) employs the $\sinh^{-1}$ function to depict rapid activation overpotential changes, albeit with potential numerical instabilities at high current densities. (14) introduces a rigidity factor, connecting the logarithm of current density to electrode characteristics and potentially simplifying reaction kinetics. These equations provide a balance between detailed accuracy and computational efficiency, vital for the effective evaluation of model performance.

(16) and (17) are selected for their straightforward yet comprehensive modelling capability, expedite and refine computation, critical for model assessment. (16) directly relates current to total system resistance, mapping out voltage variations across components. Concurrently, (19) evaluates membrane resistance considering membrane thickness and conductivity, vital for detailed energy loss analysis in electrolyzer systems.

Lastly, (22) and (23) effectively model concentration overpotentials. (22) is logarithmic formulation responsively mirrors concentration variations due to mass transport limits in electrochemical processes. (23) introduces a power-law dynamic to address non-linear outcomes at elevated currents, ensuring alignment with practical PEMWE operational scenarios and boosting the model's application relevance.

In the development of overpotential models for PEM water electrolysis, the inclusion of factors such as bubble overpotential is not universally necessary. This exclusion depends on the specific focus of the study and the anticipated operational conditions of the system. In scenarios where the primary overpotentials activation, ohmic, and concentration predominantly influence system performance, incorporating bubble overpotential may introduce redundancy. Often, the effects attributed to bubbles are implicitly accounted for within the concentration overpotential, particularly when models are calibrated with experimental data in specified operational ranges. By simplifying the model to exclude less impactful factors, computational efficiency is enhanced, allowing a sharper focus on the most critical elements that determine the electrolyzer's efficiency and effectiveness.

Table 5
Constant parameters for PEMWE model simulation and benchmarking.

Parameters	Value	Unit	Used in Eq
Standard reversible voltage $V_{rev,s}$	1.229	Volts	(10)
Universal gas constant R	8.314	J/(mol K)	(10) (13) (14) (22)
Faraday's constant F	96 485	C/mol	(10) (13) (14) (22)
Water activity α_{H_2O}	1	N/A	(10)
Temperature T	Variable	K	(10) (13) (14)
Pressure P	1.5	atm	(13) (16) (23)
Hydrogen pressure P_{H_2}	1	atm	(10)
Oxygen Pressure P_{O_2}	1	atm	(10)
Electrolyte conductivity $\mho$	1	S/m	(19)
stoichiometric coefficient z	2	N/A	(13) (14) (21) (22) (24)

4.1. Estimation of model overpotential parameters

For evaluating PEMWE models M_1 to M_8, the estimation of the key parameters are essential in simulation and benchmarking. These parameters listed in Tables 5 and 6[1] are critical across (10) to (24) and influence the accuracy and performance of the simulations by specifying their units and equations of application.

As a result of a better understanding of parameters, it is possible to simulate real-world conditions more accurately and enhance the design of the PEMWE system. The use of a Genetic Algorithm (GA) can facilitate parameter estimation, allowing the model to reflect real-life scenarios more accurately. Setting up a fitness function in GA for PEMWE systems minimizes differences between model outputs and experimental data, involving meticulous parameter adjustments like membrane thickness and electrolyte concentration. Iterative adjustments optimize PEMWE models, which are validated against additional datasets to ensure accuracy and reliability. This tailored approach balances computational efficiency and accuracy, vital for real-time operations or precise applications.

The objective function for each of the models (M_1 to M_8) is aimed at minimizing the sum of squared differences between experimentally measured and model-predicted voltages. This optimization method, particularly well-suited to addressing complex problems characterized by multiple local minima, is implemented in MATLAB to enhance computational efficiency and reproducibility [72]. The objective function is expressed by

$$J = \sum_{i=1}^{n} \left(V_i - M_k(p_k)\right)^2 \tag{33}$$

where V_i is the experimental voltage at the ith data point. $M_k(p_k)$ is the voltage predicted by model M_k using parameters p_k at the ith data point for $k = 1, 2, \ldots, 8$. The total data points are n.

[1] *These parameters are estimated by GA; however, parameters may have various amount in different equations in a model due to operational modes like temperature or pressure in different situations.

Table 6
Estimated parameters for PEMWE model simulation and benchmarking.

Parameters	M_1	M_2	M_3	M_4	M_5	M_6	M_7	M_8
Exchange current density i_0*	$1.2e^{-3}$	$1.4e^{-3}$	$1.5e^{-3}$	$1.6e^{-3}$	$1.7e^{-3}$	$1.8e^{-3}$	$1.9e^{-3}$	$2.3e^{-3}$
Limiting current density i_l* A/m^2	1.63	1.79	1.69	1.77	2	1.53	1.78	1.91
The effective surface area γ_j* m^2/s	$2e^{-5}$	$5e^{-6}$	$1e^{-5}$	$2.5e^{-5}$	$2.6e^{-5}$	$7.5e^{-5}$	$2.8e^{-5}$	$2.9e^{-5}$
Charge Transfer Coefficient α*	0.08	1.14	0.18	0.2	2.19	0.27	1.32	0.35
Concentration constant β*	0.7	5.2	3.1	2.8	3.3	4.6	3.9	3.8
Concentration constants β_1*	0.01	0.18	0.23	0.36	0.23	0.52	0.06	0.41
Concentration constants β_2*	0.17	0.47	0.94	0.66	0.83	0.48	0.37	0.54
Thickness of the membrane θ*	185.3	125.6	263.9	307.4	139.2	98.4	317.8	349.6
Membrane humidification λ*	52.4	33.7	78.5	58.9	97.3	99.4	38.7	67.1
Ohmic resistance Ω_M*	0.13	0.05	0.1	0.34	0.21	0.24	0.36	0.12
Ohmic resistance Ω_E*	0.32	0.19	0.14	0.23	0.08	0.23	0.31	0.45

Table 7
PEMWE technical specifications.

Parameters	Specifications
Model	QLC-1000
Number of cells N	4
Operational current range	0–36 A
Active area	50 cm^2
Operational voltage range	DC 12–15 V
Hydrogen production rate	1000 ml/min
Operational temperature	5–40 °C
Feed System	Gravity-fed

Optimization of the model is carried out using a Genetic Algorithm (GA), which is well suited to complex optimization problems with multiple local minima. The optimization process is initiated by randomly generating potential solutions within defined limits. Each solution undergoes evaluation, and selections are made for further breeding through methods such as tournament or roulette wheel selection. Crossover produces offspring, and mutations are introduced to increase diversity and enhance exploration of the search space. This cycle repeats until the predefined stopping criteria are met, such as reaching a maximum number of generations or observing minimal changes in the best solution. Constraints are applied to ensure that the solutions remain realistic and relevant [73].

5. PEM electrolyzer test bench and operational conditions

The study uses a PEMWE test bench equipped with current, voltage, and gas flow measurement instruments, integrated with software for data handling via the electrolyzer's digital controls. The system is calibrated before experiments to ensure data consistency and repeatability. After achieving steady state, data is refined to eliminate transient anomalies and then compared with electrochemical models to assess the PEMWE system's performance and pinpoint discrepancies between theoretical predictions and actual results. Fig. 5(a) shows the PEMWE test bench setup. Specific operational parameters and hydration control methods are detailed in Table 7.

Table 8 outlines the Balance of Plant (BOP) technical specifications for the electrolyzer, featuring a programmable power supply for precise input control tailored to the dynamics of PEM electrolysis. The test bench is equipped with a Labview suite for real-time data management and high-resolution flow meters to monitor hydrogen and oxygen production rates.

Fig. 5 details the key electrical components of the PEMWE test bench, which ensure both smooth operation and safety. The architecture includes a main switch that toggles between operational and standby modes, optimizing energy use and system readiness. An emergency push-button facilitates rapid shutdown in an emergency to protect both equipment and operators. Fuse protection also protects against electrical surges, which is essential for the protection of sensitive components. The power source is finely calibrated to meet PEMWE's specific energy demands, ensuring optimal performance and longevity. The precision of PEMWE test bench results hinges on maintaining strict operational conditions that mimic real-world environments for detailed system evaluation. Key to this is a stable temperature, consistently maintained at approximately 24 °C to optimize hydrogen production and minimize fluctuations. The test setup measures hydrogen flow at atmospheric pressure to maintain stable output and avoid pressure-related discrepancies. A gravity-fed water system ensures continuous water flow, preventing concentration overpotential. The bench's electrical setup prioritizes safety with streamlined controls, including a single switch-off and an emergency push-button as depicted in Fig. 5(b), ensuring operational safety and data integrity. At the heart of operations is a computer-controlled programmable power source that adjusts electrical parameters dynamically, capturing real-time data for subsequent analysis against established electrochemical models.

6. Results and discussion

The performance of various predictive models for PEMWE was assessed using four primary statistical metrics: Root Mean Error (MSE), Root Mean Squared Error (RMSE), Mean Absolute Error (MAE), and Coefficient of Determination (R^2), as outlined in Fig. 6. Based on the different models evaluated M_1 through M_8, different approaches to the simulation of PEMWE are explored, with varying degrees of mathematical integration and complexity. The performance of each model across four critical statistical measures shown in Fig. 6; model M_1 exhibited moderate performance with an MSE of 0.093, RMSE of 0.305, MAE of 0.234, and an impressive R^2 of 0.99076. Model M_4 showed the best overall performance with the lowest MSE (0.039), RMSE (0.199), and MAE (0.101), along with the highest R^2 (0.996), indicating a highly accurate model. Model M_3, designed to address complex dynamics, had the highest errors with MSE of 0.179, RMSE of 0.423, and MAE of 0.373, but still managed an R^2 of 0.982, reflecting reasonable model fit despite high variability in predictions.

While these metrics indicate that most models are quite robust, capturing the underlying dynamics of the PEMWE differences in error metrics largely demonstrate that model selection is influenced by the characteristics of the experimental data as well as the electrolyzers operational settings. Fig. 7 depicts the models' performance across the polarization curve. The line graph, representing voltage against current density, illustrates how closely each model M_1 through M_8 follows experimental data. Models M_4 and M_7 track the experimental curve closely, indicating their effective capture of the physical and chemical processes within the PEMWE under varied operating currents.

6.1. Comparison of hydrogen production

This section evaluates eight electrochemical models (HyPro1 through HyPro8) for their accuracy in predicting hydrogen generation at different current densities. 'HyPro' represents the estimated hydrogen production by each model, derived from (8), resulting in individual outputs like HyProx. The main objective is to determine which model aligns best with the test bench data, aiming to find the models'

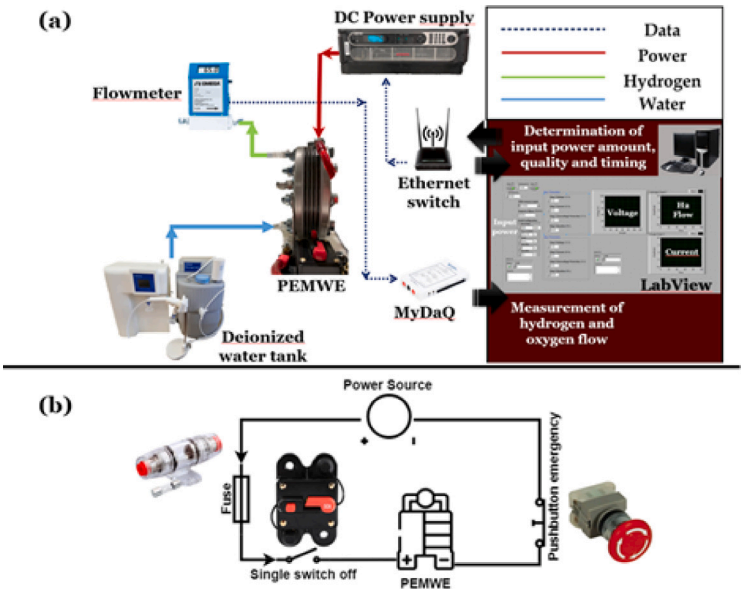

Fig. 5. (a) PEMWE test bench and its BOP, (b) schematic diagram of electrical safety and control components in PEMWE BOP.

Table 8
BOP technical specifications.

Component	Specification	Description/Function
Power supply	0–100 V and 0–100 A	Provides controlled DC power
Data acquisition	myDAQ (National Instruments) system interfaced with LabVIEW	Collects and processes real-time data from the test bench
H_2 flow	Omega FH	Volumetric emanation rates of hydrogen
Control mechanism	PC-controlled power supply	Provides control over the power delivered to the PEM electrolyzer through LabVIEW
Feed water reservoir	Elevated for gravitational flow	Stores and feeds deionized water to the electrolyzer using gravity
Temperature measurement	Precision thermocouples/sensors	Monitors and records the operational temperature of the PEM electrolyzer during the testing process

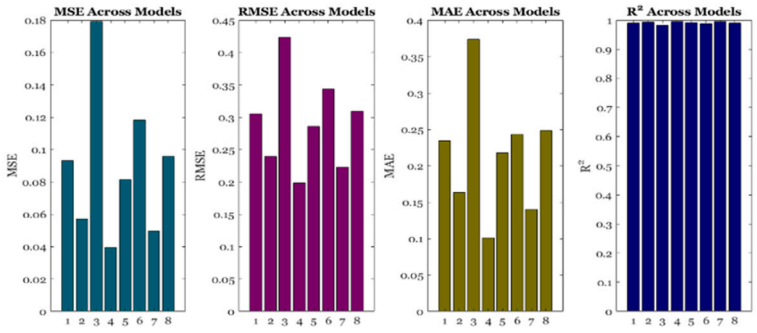

Fig. 6. Performance metrics comparison across models.

predictive capabilities for the model benchmark of PEMWE systems. This evaluation is crucial for exploring operational performance and developing appropriate EMSs. Fig. 8 displays hydrogen production rates at various current densities, juxtaposing actual data (black circles) with model predictions (coloured lines). The graph indicates that models HyPro2, HyPro4, and HyPro7 closely align with actual data, showing high accuracy, while HyPro3 and HyPro6 exhibit significant deviations, particularly at higher current densities.

Error analysis, detailed in Fig. 9, shows that M_4 consistently has the lowest error rates across all densities, highlighting its accuracy. Conversely, M_3 exhibits significant errors at higher densities, suggesting it requires refinement.

Fig. 10 measures errors in millilitres per minute (ml/min), with M_4 maintaining the lowest average error at about 14 ml/min, confirming its precision. Models M_3 and M_6, with average errors of 45 ml/min, indicate a need for adjustment to better match experimental conditions.

The analysis provided in both Figs. 9 and 10 are crucial for evaluating the relative performance of different models in consistent experimental settings. It allows identifying which models frequently deviate from observed measurements and points out the necessity for ongoing refinement. This approach is valuable for monitoring long-term trends in model performance and underscores the need for developing precise models. It also provides a critical evaluation of model performance, for

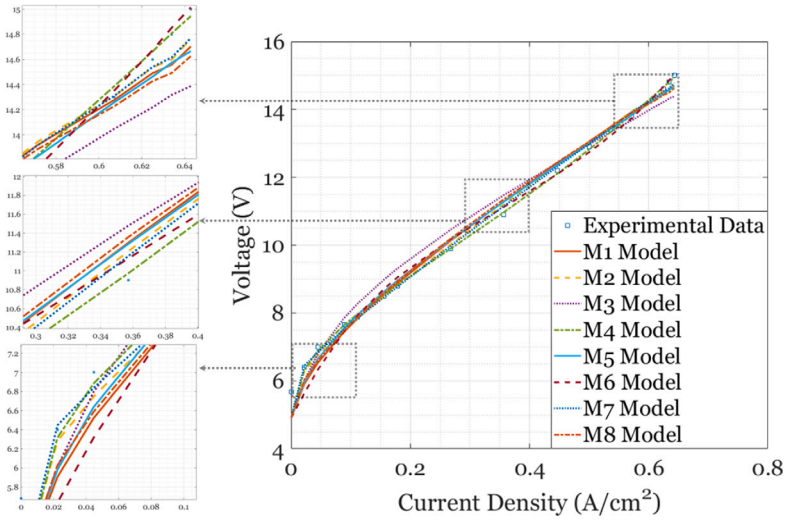

Fig. 7. Voltage–current characteristic comparison of PEMWE models with experimental data.

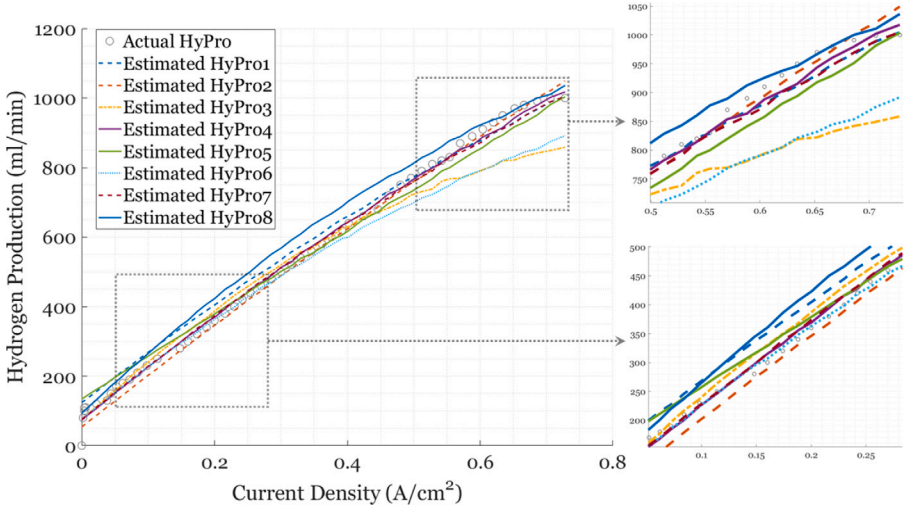

Fig. 8. Actual vs estimated hydrogen production models.

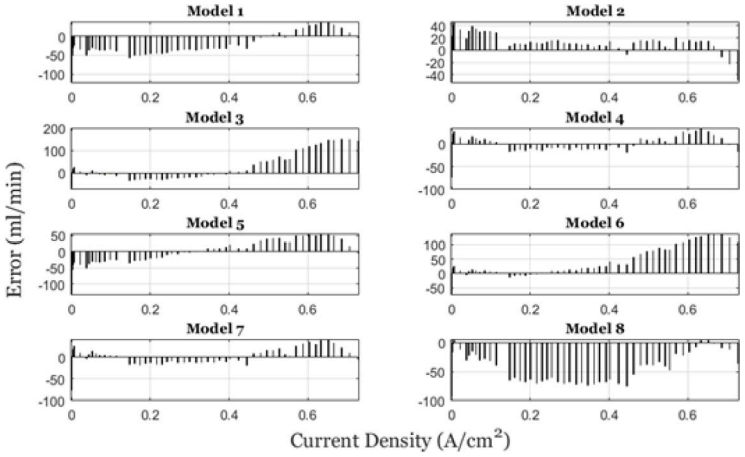

Fig. 9. Error analysis across current density for models.

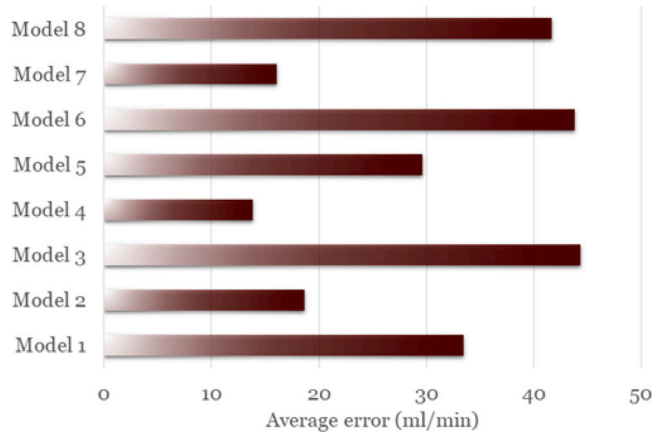

Fig. 10. Average error of model predictions for hydrogen production in PEMWEs.

identifying models like M_3 and M_3 that may need further tuning to enhance accuracy.

6.2. Comparative analysis of model complexity and performance

This section presents a comparative analysis of model complexity and performance. It enables the assessment of eight models based on their parameter configurations categorized into total, estimated, constant, and measured parameters as depicted in Fig. 11. The radar chart in this figure visually compares the models across these parameter categories to highlight their respective complexities and capabilities.

The comparison of models is categorized into four key parameter types: total, estimated, constant, and measured. The total parameters (a) encompass all parameters utilized within each model, offering a comprehensive view of the model's overall complexity. Estimated parameters (b) refer to those that are inferred rather than directly measured; a higher count of these parameters can lead to reduced predictive accuracy due to inherent uncertainties in the estimation process. Constant parameters (c), on the other hand, remain unchanged across various operational scenarios, playing a crucial role in maintaining the stability of the model's predictions. Finally, Measured parameters (d) are directly obtained from experimental data, and their inclusion can significantly enhance the model's robustness, ensuring that simulations are closely aligned with real-world operational conditions.

The analysis highlights that the selection of an appropriate model depends significantly on the balance between complexity and performance. Models with many estimated parameters might offer flexibility but at the risk of lower accuracy, while those with more measured parameters are likely more reliable but could be complex to implement. This benchmarking facilitates the choice of an optimal model for specific electrolyzer systems, aiming to improve simulation fidelity and operational efficiency.

6.3. Discussion

The discussion surrounding the performance evaluation of various predictive models for PEMWE systems reveals several critical insights into the selection and application of these models. The analysis of four primary statistical metrics (MSE, RMSE, MAE, and R^2) indicates that while models like M_4 exhibit superior overall accuracy, the choice of model must consider the specific operational and experimental conditions. The results demonstrate that models with lower error metrics are generally better suited to accurate simulations, but the variability in performance across different scenarios underscores the importance of tailoring model selection to the unique characteristics of the system being studied.

Furthermore, the comparison of hydrogen production models highlights the importance of aligning predicted data with experimental results. Models such as HyPro2, HyPro4, and HyPro7, which closely match the actual hydrogen production data, suggest that accurate modelling of PEMWE systems requires a careful balance between complexity and empirical validation. The deviation observed in models

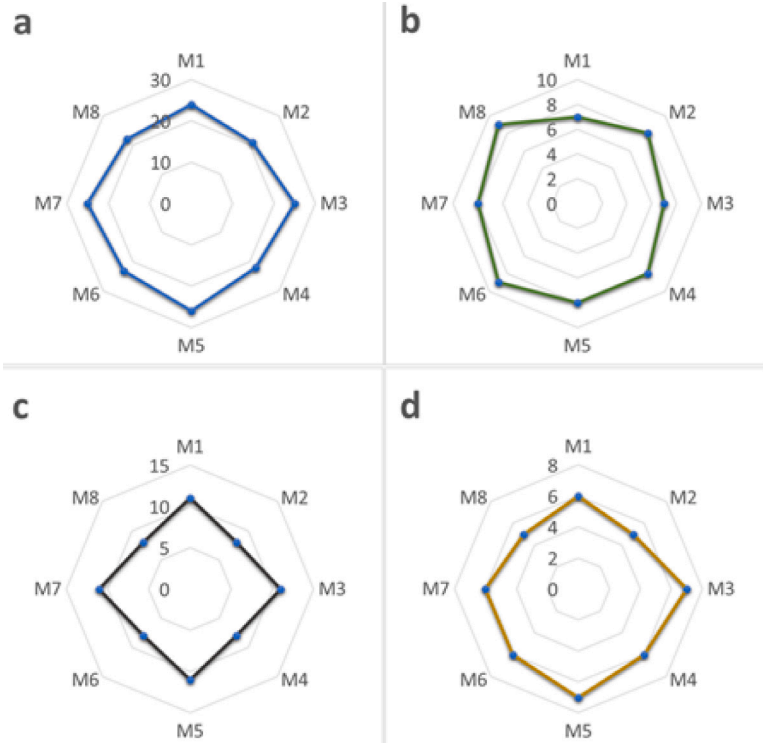

Fig. 11. Parameters comparison of models M_1 to M_8 (a) Total (b) Estimated (c) Constant (d) Measured.

like HyPro3 and HyPro6 at higher current densities indicates that further refinement is necessary to improve their predictive capabilities, particularly under more demanding operational conditions.

The discussion herein extends beyond mere model performance evaluation to explore the practical implications of the findings for real-world energy management. This study provides essential insights into selecting the most suitable models for specific applications by demonstrating how different models perform under various conditions. This serves the scientific community by outlining clear, actionable guidance and assists industry professionals in making informed decisions that enhance the operational efficiency and sustainability of PEMWE systems.

In the context of model complexity and performance, the radar chart comparison of parameters provides a comprehensive view of each model's strengths and weaknesses. Models with a higher count of measured parameters tend to be more robust and accurate, as they align more closely with real-world conditions. However, the increased complexity associated with these models may present challenges in implementation. This discussion emphasizes that achieving an optimal balance between model simplicity and accuracy is crucial for effective energy management in PEMWE systems, and this benchmarking approach serves as a valuable tool for guiding model selection and refinement.

7. Conclusion

An extensive benchmarking of PEMWE models is undertaken in this study, proposing grey-box approach, and employing a novel method for comparing submodels in different configurations. The analysis singles out Model M_4 for its exceptional performance, demonstrating the lowest error metrics like MSE, RMSE, MAE, and R^2, affirming its strong alignment with experimental data and high reliability in forecasting hydrogen production rates.

While Model M_4 proves superior in many scenarios, this study reveals that no single model achieves universal applicability. Certain models, such as M_3, exhibit elevated error rates at higher current densities, suggesting a need for targeted refinement to enhance their predictive accuracy. This variability underscores the necessity of customizing model selection based on the specific operational requirements and experimental conditions of the PEMWE systems in question.

Additionally, the research identifies the importance of a systematic approach to selecting and validating PEMWE the most appropriate models for specific applications. It illustrates that choosing the right model involves balancing computational simplicity with the depth of accuracy needed for effective energy management. In addition to facilitating the selection of the most appropriate model for specific applications, this comprehensive comparison provides a foundational framework for the development of scalable and efficient energy management strategies and power allocation.

Conclusively, the insights garnered from this benchmarking provide valuable guidelines for future enhancements in model precision and practical deployment. Beyond enriching the theoretical landscape of PEMWE modelling, this study bridges the gap between complex modelling and industrial applications, offering actionable knowledge that can significantly contribute to the advancement of sustainable hydrogen production technologies and the optimization of PEMWE systems for energy management.

CRediT authorship contribution statement

Ashkan Makhsoos: Writing – original draft, Visualization, Methodology, Formal analysis, Data curation, Conceptualization. **Mohsen Kandidayeni:** Writing – review & editing, Validation, Supervision, Data curation. **Meziane Ait Ziane:** Writing – review & editing, Writing – original draft, Validation, Formal analysis, Data curation. **Loïc Boulon:** Writing – review & editing, Supervision, Project administration, Funding acquisition. **Bruno G. Pollet:** Writing – review & editing, Supervision.

Declaration of competing interest

The authors declare that they have no known competing financial interests or personal relationships that could have appeared to influence the work reported in this paper.

Acknowledgement

This work was supported in part by the Natural Sciences and Engineering Research Council of Canada (NSERC) (2018-06527).

Data availability

The data that has been used is confidential.

References

[1] Peter J B. Introduction to energy transition: Climate action and circularity. Energy Trans: Clim Action Circ. Am Chem Soc 2022;1–20.
[2] Megía PJ, Vizcaíno AJ, Calles JA, Carrero A. Hydrogen production technologies: from fossil fuels toward renewable sources. A mini review. Energy Fuels 2021;35(20):6403–16415.
[3] Colangelo G, Spirto G, Milanese M, Risi AD. Hydrogen production from renewable energy resources: A case study. Energy Convers Manage 2024;311:118532.
[4] Moghadari M, Kandidayeni M, Boulon L, Chaoui H. Minimizing the operating cost of a hybrid multi-stack fuel cell vehicle based on a predictive hierarchical strategy. In: 2023 IEEE Vehicle Power and Propulsion Conference (VPPC). 2023, p. 1–5.
[5] Yamchi HB, Kandidayeni M, Kelouwani S, Boulon L. Analytical modelling and experimental validation of proton exchange membrane electrolyser for hydrogen production. Int J Hydrog Energy 2017;42(2):1366–74.
[6] Kim J, Qi M, Kim M, Lee J, I. Lee IM. Biogas reforming integrated with PEM electrolysis via oxygen storage process for green hydrogen production: From design to robust optimization. Energy Convers Manage 2022;251:115021.
[7] Salari A, Shakibi H, Habibi A, Hakkaki-Fard A. Optimization of a solar-based PEM methanol/water electrolyzer using machine learning and animal-inspired algorithms. Energy Convers Manage 2023;283:116876.
[8] Zhang X, Zeng R, Du T, He Y, Tian H, Mu K, Liu X, Li H. Conventional and energy level based exergoeconomic analysis of biomass and natural gas fired polygeneration system integrated with ground source heat pump and PEM electrolyzer. Energy Convers Manage 2019;195:313–27.
[9] Song S H, Luo, Huang H, Deng B, Ye J. Solar-driven hydrogen production: Recent advances challenges and future perspectives. ACS Energy Lett 2022;7(3):1043–65.
[10] Aftab A, Hassanpouryouzband A, Xie Q, Machuca L, Sarmadivaleh M. Toward a fundamental understanding of geological hydrogen storage. Ind Eng Chem Res 2022;61(9):3233–53.
[11] Bellotti D, Rivarolo M, Magistri L. A comparative techno-economic and sensitivity analysis of power-to-X processes from different energy sources. Energy Convers Manage 2022;260:115565.
[12] Lee H, Lee B, Byun M, Lim H. Economic and environmental analysis for PEM water electrolysis based on replacement moment and renewable electricity resources. Energy Convers Manage 2020;224:113477.
[13] Panigrahy B, Narayan K, Ramachandra Rao B. Green hydrogen production by water electrolysis: A renewable energy perspective. Mater. Today: Proc 2022;67:1310–4.
[14] Vivas F, Segura F, Andújar J, Caparrós J. A suitable state-space model for renewable source-based microgrids with hydrogen as backup for the design of energy management systems. Energy Convers Manage 2020;219:113053.
[15] Wang J, Cai S, Chen R, Tu Z, Li S. Operation strategy optimization of an integrated proton exchange membrane water electrolyzer and batch reverse osmosis desalination system powered by offgrid wind energy. Energy Convers Manage 2024;22:100607.
[16] Correia L, Schwabe O, Almeida N. Speed of innovation diffusion in green hydrogen technologies. In: 15th WCEAM Proceedings. Springer; 2022, p. 101–11.
[17] Tebibel H. Methodology for multi-objective optimization of wind turbine/battery/electrolyzer system for decentralized clean hydrogen production using an adapted power management strategy for low wind speed conditions. Energy Convers Manage 2021;238:114125.
[18] Makhsoos A, Kandidayeni M, Pollet BG, Boulon L. A perspective on increasing the efficiency of proton exchange membrane water electrolyzers– a review. Int J Hydrog Energy 2023;48(41):15341–70.
[19] Eikeng E, Makhsoos A, Pollet BG. Critical and strategic raw materials for electrolysers, fuel cells, metal hydrides and hydrogen separation technologies. Int J Hydrog Energy 2024;71:433–64.

[20] Bermudez SEJM, Pavan F. Electrolysers technology deep dive, more efforts needed. 2023.
[21] Li Y, Deng X, Zhang T, Liu S, Song L, Yang F, Ouyang M, Shen X. Exploration of the configuration and operation rule of the multi-electrolyzers hybrid system of large-scale alkaline water hydrogen production system. Appl Energy 2023;331:pp.120413.
[22] Kafetzis A, Ziogou C, Panopoulos KD, Papadopoulou S, Seferlis P, Voutetakis S. Energy management strategies based on hybrid automata for islanded microgrids with renewable sources, batteries and hydrogen. Renew Sustain Energy Rev 2020;134:pp.110118.
[23] Salehmin M, Husaini T, Goh J, Sulong A. High-pressure PEM water electrolyser: A review on challenges and mitigation strategies towards green and low-cost hydrogen production. Energy Convers Manage 2022;268:115985.
[24] Qian X, Kim K, Jung S. Multiphase, multidimensional modeling of proton exchange membrane water electrolyzer. Energy Convers Manage 2022;268:116070.
[25] Folgado F, González I, Calderón A. Simulation platform for the assessment of PEM electrolyzer models oriented to implement digital Replicas. Energy Convers Manage 2022;267:115917.
[26] Lamy C, Millet P. A critical review on the definitions used to calculate the energy efficiency coefficients of water electrolysis cells working under near ambient temperature conditions. J Power Sources 2020;447:pp.227350.
[27] Olivier P, Bourasseau C, Bouamama PB. Low-temperature electrolysis system modelling: A review. Renew Sustain Energy Rev 2017;78:280–300.
[28] Falcão D, Pinto A. A review on PEM electrolyzer modelling: Guidelines for beginners. J Cleaner Product 2020;261:pp.121184.
[29] Hernandez-Gomez A, Ramirez V, Guilbert D. Investigation of PEM electrolyzer modeling: Electrical domain, efficiency, and specific energy consumption. Int J Hydrog Energy 2020;45(29):14625–39.
[30] Majumdar A, Haas M, Elliot I, Nazari S. Control and control-oriented modeling of PEM water electrolyzers: A review. Int J Hydrog Energy 2023;48:30621–41.
[31] Du B, Zhu S, Zhu W, Lu X, Li Y, Xie C, Zhao B, Zhang L, Xu G, Song J. Energy management and performance analysis of an off-grid integrated hydrogen energy utilization system. Energy Convers Manage 2024;299:117871.
[32] HassanzadehFard H, Tooryan F, Collins ER, Jin S, Ramezani B. Design and optimum energy management of a hybrid renewable energy system based on efficient various hydrogen production. Int J Hydrog Energy 2020;45(55):30113–28.
[33] Calderónand A, Calderón M. Management of a PEM electrolyzer in hybrid renewable energy systems. Fuzzy Model Contr: Theory Appl 2014;217–34.
[34] Li Y, Shang Z, Peng F, Zhao Y, Ren L. Improved control-oriented polarization characteristic modeling for proton exchange membrane water electrolyzer with adaptive hunting game based metaheuristic optimization. Energy Convers Manage 2024;305:118264.
[35] Chandesris M, Médeau V, Guillet N, Chelghoum S, Thoby D, Fouda-Onana F. Membrane degradation in PEM water electrolyzer: Numerical modeling and experimental evidence of the influence of temperature and current density. Int J Hydrog Energy 2015;40(3):353–1366.
[36] Kim H, Park M, Lee KS. One-dimensional dynamic modeling of a high-pressure water electrolysis system for hydrogen production. Int J Hydrog Energy 2013;38:2596–609.
[37] Abdin Z, Webb CJ, Gray EM. Modelling and simulation of a proton exchange membrane (PEM) electrolyser cell. Int J Hydrog Energy 2015;40(39):13243–57.
[38] Gaspar FJF, Godoy AJC, Pérez IG, Godoy MC, Calero JMP, Martín DO. Design of a simulation platform to test the suitability of different PEM electrolyzer models to implement digital replicas. In: International Conference on Simulation and Modeling Methodologies, Technologies and Applications. 2021.
[39] R. García-Valverde NE, Urbina A. Simple PEM water electrolyser model and experimental validation. Int J Hydrog Energy 2012;37:1927–38.
[40] Atlam O, Kolhe M. Equivalent electrical model for a proton exchange membrane (PEM) electrolyser. Energy Convers Manage 2011;52(8):2952–7.
[41] Aouali FZ, Becherif M, Ramadan HS, Emziane M, Khellaf A, Mohammedi K. Analytical modelling and experimental validation of proton exchange membrane electrolyser for hydrogen production. Int J Hydrog Energy 2017;42(2):1366–74.
[42] Marangio F, Santarelli M, Calì M. Theoretical model and experimental analysis of a high pressure PEM water electrolyser for hydrogen production. Int J Hydrog Energy 2009;34(3):1143–58.
[43] Sezer N, Bayhan S, Fesli U, Sanfilippo A. A comprehensive review of the state-of-the-art of proton exchange membrane water electrolysis. Mater Sci Energy Technol 2025;8:44–65.
[44] Kumar SS, Lim H. An overview of water electrolysis technologies for green hydrogen production. Energy Rep 2022;8(19):13793–813.
[45] Hancke R, Holm T, Ulleberg Ø. The case for high-pressure PEM water electrolysis. Energy Convers Manage 2022;261:115642.
[46] Liu G, Dastafkan K, Zhao C. Electrochemical water splitting. Heterog Catal: Adv Design, Charact Appl 2021;2:533–55.
[47] Chen J, Sun Y, Hu D, Yao H, Shen X, Zhang C, Lv H. Performance modeling and mechanism study of proton exchange membrane water electrolyzer coupled with water electroosmosis. Energy Convers Manage 2024;315:118753.
[48] Raveendran A, Chandran M, Dhanusuraman R. A comprehensive review on the electrochemical parameters and recent material development of electrochemical water splitting electrocatalysts. RSC Adv 2023;13:3843–76.
[49] Rodríguez NDJ, Luxa A, Jürgensen L. Adaptation and application of a polarisation curve test protocol for a commercial pem electrolyser on cell and stack level. Acta Mech Autom 2023;17(3):395–404.
[50] Makhsoos A, Kandidayeni M, Boulon L, Pollet BG, Kelouwani S. Evaluation of high-efficiency hydrogen production from solar energy using artificial neural network at the Université du Québec à Trois-Rivières. In: 2022 IEEE Vehicle Power and Propulsion Conference (VPPC). 2022, p. 1–4.
[51] Järvinen L. Automized parametrization of PEM and alkaline water electrolyzer polarisation curves. Int J Hydrog Energy 2022;47(75):31985–2003.
[52] Görgün H. Dynamic modelling of a proton exchange membrane (PEM) electrolyzer. Int J Hydrog Energy 2006;31(1):29–38.
[53] Crespi E, Guandalini G, Mastropasqua L, S. Campanari JB. Experimental and theoretical evaluation of a 60 kW PEM electrolysis system for flexible dynamic operation. Energy Convers Manage 2023;277:116622.
[54] Choi P, Bessarabov DG, Datta R. A simple model for solid polymer electrolyte (SPE) water electrolysis. Solid State Ion 2004;175:535–9.
[55] Abomazid AM, El-Taweel NA, Farag HEZ. Novel analytical approach for parameters identification of PEM electrolyzer. IEEE Trans Ind Inf 2022;18(9):5870–81.
[56] Laoun B, Khellaf A, Naceur MW, Kannan AM. Modeling of solar photovoltaic-polymer electrolyte membrane electrolyzer direct coupling for hydrogen generation. Int J Hydrog Energy 2016;44(24):10120–35.
[57] Schalenbach M, Carmo M, Fritz DL, Mergel J, Stolten D. Pressurized PEM water electrolysis: Efficiency and gas crossover. Int J Hydrog Energy 2013;38(35):14921–33.
[58] Mohamed B, Alli B, Ahmed B. Using the hydrogen for sustainable energy storage: Designs, modeling, identification and simulation membrane behavior in PEM system electrolyser. J Energy Storage 2016;7:270–85.
[59] Maggio G, Recupero V, Pino L. Modeling polymer electrolyte fuel cells: an innovative approach. J Power Sources 2001;101(2):275–86.
[60] Correa G, Marocco P, Muñoz P, Falagüerra T, Ferrero D, Santarelli M. Pressurized PEM water electrolysis: Dynamic modelling focusing on the cathode side. Int J Hydrog Energy 2022;47(7):4315–27.
[61] Jing K, Liu C. Online observer of the voltage components of the PEM electrolyzer based on the time-varying linearization of the semi-empirical model. Energy Rep 2023;9:99–307.
[62] Ursúa A, Sanchis P. Static–dynamic modelling of the electrical behaviour of a commercial advanced alkaline water electrolyser. Int J Hydrog Energy 2012;37(24):18598–614.
[63] Wang B, Ni M, Zhang S, Liu Z, Jiang S, Zhang L, Zhou F, Jiao K. Two-phase analytical modeling and intelligence parameter estimation of proton exchange membrane electrolyzer for hydrogen production. Renew Energy 2023;211:202–13.
[64] Agbli KS, Péra MC, Hissel D, Rallières O, Turpin C, Doumbia I. Multiphysics simulation of a PEM electrolyser: Energetic macroscopic representation approach. Int J Hydrog Energy 2011;36(2):1382–98.
[65] Afshari E, Khodabakhsh S, Jahantigh N, Toghyani S. Performance assessment of gas crossover phenomenon and water transport mechanism in high pressure PEM electrolyzer. Int J Hydrog Energy 2017;46(19):11029–40.
[66] Ojong ET, Kwan JTH, Nouri-Khorasani A, Bonakdarpour A, Wilkinson DP, Smolinka T. Development of an experimentally validated semi-empirical fully-coupled performance model of a PEM electrolysis cell with a 3-D structured porous transport layer. Int J Hydrog Energy 2017;42(41):25831–47.
[67] Gabrielli P, Flamm B, Eichler A, Gazzani M, Lygeros J, Mazzotti M. Modeling for optimal operation of PEM fuel cells and electrolyzers. In: IEEE 16th International Conference on Environment and Electrical Engineering (EEEIC). 2016, p. 1–7.
[68] Zhang H, Su S, Lin G, Chen J. Efficiency calculation and configuration design of a PEM electrolyzer system for hydrogen production. Int J Electrochem Sci 2012;7(5):4143–57.
[69] Lebbal ME, Lecœuche S. Identification and monitoring of a PEM electrolyser based on dynamical modelling. Int J Hydrog Energy 2009;34(14):5992–9.
[70] Nouri-Khorasani A, Ojong ET, Smolinka T, Wilkinson DP. Model of oxygen bubbles and performance impact in the porous transport layer of PEM water electrolysis cells. Int J Hydrog Energy 2017;42(48):28665–80.
[71] Zhou H, Meng K, Chen W, Chen B. Exploratory research on bubbles migration behavior and mass transfer capacity evaluation of proton exchange membrane water electrolyzer based on a volume of fluid-coupled electrochemical model. Energy Convers Manage 2023;290:117217.
[72] Singh A, Khamparia A. A hybrid whale optimization-differential evolution and genetic algorithm based approach to solve unit commitment scheduling problem: WODEGA. Sustain Comput: Inform Syst 2020;28:100442.
[73] MathWorks. Optimization toolbox. (2022). The MathWorks inc.. Sustain Comput: Inform Syst 2020.